Image potential for an electron near an impenetrable surface

Xiang-Yang Zheng and R. H. Ritchie
Health and Safety Research Division, Oak Ridge National Laboratory, P.O. Box 2008, Oak Ridge, Tennessee 37831-6123
and Department of Physics, University of Tennessee, Knoxville, Tennessee 37996
(Received 23 July 1990)

A self-energy formalism is used to determine the quantal image potential for an electron near an impenetrable solid surface. The electron is considered to be in a Coulombic potential outside a repulsive wall. The complete, orthonormal basis set of wave functions for an electron in such a model potential is employed in the calculation of the image potential.

The polarization induced by a charged particle near a polarizable medium acts back on the charge and gives rise to an attractive potential. The classical image potential is $V_{\rm cl}=-ZQ^2/z$ for a charge Q at fixed distance z from a planar surface, where $Z=(\epsilon_0-1)/4(\epsilon_0+1)$ and ϵ_0 is the static dielectric constant of the bulk medium. The unphysical divergence of $V_{\rm cl}$ as $z\to 0$ is removed in a quantum-mechanical treatment. The properties of the interaction potential for an electron near a solid surface are important to interpretation of experimental results obtained from electron-based surface spectroscopies such as the low-energy electron diffraction (LEED) and reflection-electron-energy-loss (REEL) spectroscopy. A detailed knowledge of the interaction between a charge and a solid surface is also important for the analysis of surface states.[1-4]

Various approaches[5-10] to the quantum-mechanical calculation of the image potential have been made. The concept of self-energy in the quantum-mechanical many-particle theory is well suited for the image-potential problem. A rigorous approach to the self-energy should employ the fully screened Coulomb interaction propagator which contains information about single particle electron-hole excitations as well as collective electronic excitations, which in this case are the surface plasmons.[10] Many authors have used the present Hamiltonian to represent the surface plasmon field because of its analytical simplicity and the fact that it represents the image potential at large distances from the surface. Quantum theories in this framework give important dynamical corrections to the classical image potential due to the effects of dispersion of surface excitations and recoil due to the exchange of virtual quanta between the charge and the surface. We adopt a self-energy formalism[7] for determining the image potential in this connection. This simple yet powerful approach gives the complex self-energy for a charged particle near a solid surface with arbitrary trajectory. The real part of the self-energy gives the image potential while the imaginary part characterizes the properties of the energy loss of the particle to the solid medium. Application of this formalism has been made to the investigations of van der Waals forces between atoms,[11] the energy transfer between a moving atom and a solid surface,[12] and image-potential-induced surface states.[3]

We begin with the review of this theory. Consider a charged particle projectile interacting with a many-body target. The ground-state energy shift due to the interaction of the particle with the target in second-order perturbation theory is given by

$$\Delta E_0=\sum_n\sum_k \frac{|\langle\Psi_0\varphi_0|V|\Psi_k\varphi_n\rangle|^2}{E_0-E_n+\mathcal{E}_0-\mathcal{E}_k+i\delta}\ , \tag{1}$$

where $|\Psi_k\varphi_n\rangle=|\Psi_k\rangle|\varphi_n\rangle$ is the state wave vector of the noninteracting system with $|\varphi_n\rangle$ the state vector of the charged particle corresponding to the energy E_n, $|\Psi_k\rangle$ that of the many-particle target with energy $\mathcal{E}_k$, and δ is a positive infinitesimal. For an N-particle target the interaction energy $V=\sum_i^N V(\mathbf{r}-\mathbf{r}_i)$, where $\mathbf{r}$ is the projectile coordinate and $\mathbf{r}_i$ is the coordinate of the ith target particle. It is assumed that the energy shift is related to the spatially dependent self-energy $\Sigma_0(\mathbf{r})$ through

$$\Delta E_0=\int\langle\varphi_0|\mathbf{r}\rangle\Sigma_0(\mathbf{r})\langle\mathbf{r}|\varphi_0\rangle d^3r\ . \tag{2}$$

An expression for $\Sigma_0(\mathbf{r})$ is obtained by equating the integrands of Eqs. (1) and (2) and dividing the resulting equation by $|\langle\mathbf{r}|\varphi_0\rangle|^2$, yielding

$$\Sigma_0(\mathbf{r})=\sum_n\sum_k \frac{\langle\mathbf{r}|\varphi_n\rangle}{\langle\mathbf{r}|\varphi_0\rangle}\frac{\langle\Psi_0|V|\Psi_k\rangle\langle\varphi_n\Psi_k|V|\varphi_0\Psi_0\rangle}{E_0-E_n+\mathcal{E}_0-\mathcal{E}_k+i\delta}\ . \tag{3}$$

A systematic generalization of this formalism to include higher-order corrections to the self-energy has been made.[13]

In the following we present an application of Eq. (3) adopting the surface plasmon model for the response function of the surface and using an electron basis set obtained from the Coulombic potential. This should give a good first approximation to the real image potential experienced by an electron near the surface.

It is known[5] that the long-range forces experienced by a charge external to a solid surface and not closer than an Å or so may be considered as due to the interaction between the charge and the virtual excitation of the surface modes, i.e., surface plasmon in metals, since the fields due to bulk electronic excitations extend only a few atomic

units beyond the surface. In this simple scheme of interaction the dynamical properties of the medium are codified in the response of the surface-plasmon field. However, we may also include approximately the effect of single electronic excitations by employing the so-called surface-plasmon–pole dispersion relation.[6] The interaction energy for a system of an electron and the surface excitations can be approximated as

$$V=\sum_{\kappa}\alpha_{\kappa}e^{-\kappa|z|}e^{i\kappa\cdot\rho}(a^{\dagger}_{-\kappa}+a_{\kappa}) , \tag{4}$$

where κ is a vector parallel to the surface and $a^{\dagger}_{-\kappa}$ and a_{κ} are creation and annihilation operators, respectively. The constant α_{κ} is given by $\alpha_{\kappa}^2=\pi e^2\hbar\omega_s^2/L^2\kappa\omega_{\kappa}$, where L^2 is the area of the surface, ω_{κ} is the surface plasmon frequency, and its dispersionless limit is given by $\omega_s=\omega_p/\sqrt{2}$, where $\omega_p=(4\pi n_0e^2/m)^{1/2}$ is the bulk plasmon frequency of an electron gas of density n_0.

Assuming translational invariance parallel to the surface, we may take the electron wave functions as products of plane waves along the surface and state vectors $\langle z|n\rangle$ associated with the motion of the electron normal to the surface:

$$\langle \mathbf{r}|\varphi_n\rangle=\frac{1}{L}e^{i\mathbf{P}\cdot\rho}\langle z|n\rangle , \tag{5}$$

where (ρ,z) is the coordinate of the electron. Substituting Eqs. (4) and (5) into Eq. (3) we arrive at

$$\Sigma_0(z)=\sum_n\sum_{\kappa}\frac{\langle z|n\rangle}{\langle z|0\rangle}\times\frac{\alpha_{\kappa}^2e^{-\kappa z}\langle n|e^{-\kappa|z|}|0\rangle}{\varepsilon_0-\varepsilon_n+\frac{\hbar^2}{2m}(2\mathbf{P}_0\cdot\boldsymbol{\kappa}-\kappa^2)-\hbar\omega_{\kappa}+i\delta} , \tag{6}$$

where $\mathbf{P}_0$ is the initial momentum of the electron parallel to the surface and ε_n is the energy corresponding to $|n\rangle$. For simplicity we will consider the case of $\mathbf{P}_0=0$ only in this paper. The case for $\mathbf{P}_0\neq 0$ will be discussed elsewhere.[14] The summation over κ in Eq. (6) can be converted into an integration. We extend the summation over κ to an infinite range of values in the following calculation. $\Sigma_0(z)$ is manifestly real for $\mathbf{P}_0=0$ since it corresponds to the lowest energy state of the system. When $\mathbf{P}_0\neq 0$, $\mathrm{Im}(\Sigma_0)$ describes the damping of the state $\langle \mathbf{r}|\varphi_n\rangle$ due to interactions with the target.

The orthornormal basis set of wave functions for the motion of the electron normal to the surface can be generated from the one-body Schrödinger equation

$$-\frac{\hbar^2\nabla^2}{2m}\langle z|n\rangle+\mathcal{V}\langle z|n\rangle=\varepsilon_n\langle z|n\rangle . \tag{7}$$

The potential $\mathcal{V}$ is actually the local self-energy of the charge given in Eq. (3). Therefore, a self-consistent calculation should be carried out to find both the self-energy and the wave function of the charged particle. However, for the purpose of determining the self-energy in a perturbation-theoretic approach, the classical image potential may be a reasonable first approximation to $\mathcal{V}$. We then take

$$\mathcal{V}=\begin{cases}-\dfrac{e^2}{4z}, & z>0\\ \infty, & z=0 .\end{cases} \tag{8}$$

This model potential is relevant to the case of an electron outside of a metal surface for which there is an energy gap that contains the vacuum level in the direction normal to the surface. Surfaces of Cu(001) and Ag(001) are examples. The electron does not have enough energy to penetrate into the bulk, but the image potential seen by an electron may be strong enough to trap it and thus lead to electron surface states,[1–3] which have been shown to exist by LEED and inverse photoemission experiments.[4]

The solutions of Eq. (7) are just the one-dimensional Coulombic wave functions. For discrete states the eigenenergy is

$$\varepsilon_n=-\frac{me^4}{32\hbar^2n^2} \tag{9}$$

and the Coulomb wave function is given by[15]

$$\langle z|n\rangle=C_nZe^{-z/4na_0}F\left[-n+1,2\frac{z}{2na_0}\right] , \tag{10}$$

where $C_n=z(4na_0)^{-3/2}$ and $F(a,c,z)$ is the confluent hypergeometric function; a_0 here is the Bohr radius. The matrix in Eq. (6) is given by[15]

$$\langle n|e^{-\kappa z}|0\rangle=C_0C_n\frac{2}{(1/4a_0+\kappa+1/4na_0)^3}\times\left[\frac{n(1/4a_0+\kappa)-1/4a_0}{n(1/4a_0+\kappa)+1/4a_0}\right]^{n-2} . \tag{11}$$

For the continuum state, we make the following substitution:

$$\frac{\langle n|e^{-\kappa z}|0\rangle}{C_n}\Longleftrightarrow\frac{\langle E|e^{-\kappa z}|0\rangle}{C_E}$$

under the change $n\rightarrow i\eta$, where $C_E=(\pi k/L)(1-e^{-2\pi n})^{-1}$ and $k=\sqrt{2mE}/\hbar^2$, $\eta=1/4ka_0$.

To evaluate Eq. (6), we need to know the dispersion relation of the surface plasmons. We adopt the surface-plasmon–pole dispersion relation[6]

$$\omega_{\kappa}=(\omega_s^2+\alpha\kappa+\beta\kappa^2+\kappa^4/4)^{1/2} , \tag{12}$$

where $\alpha=\sqrt{(3/5)}v_F\omega_s$ with v_F the Fermi velocity. The coefficient $\beta=0.0026+2.6798/r_s^{1.85}$, where r_s is the one electron radius. This dispersion relation includes, schematically, the effects of both plasmon and electron-hole excitations.

In the numerical calculation the complex confluent hypergeometric function $F(a,c,z)$ is evaluated by matching two series expansions.[16] We have found that for $|z|<20$ the expansion

$$F(a,c,z)=1+\frac{a}{c}\frac{z}{1!}+\frac{a(a+1)}{c(c+1)}\frac{z^2}{2!}+\cdots \tag{13}$$

may be used with good accuracy, while for $|z|>10$ the asymptotic series of $F(a,c,z)$,

$$F(a,c,z)=\frac{\Gamma(c)}{\Gamma(c-a)}(-z)^{-a}G(a,a-c+1,-z)+\frac{\Gamma(c)}{\Gamma(a)}e^{z}z^{a-c}G(c-a,1-a,z)\ , \quad (14)$$

is appropriate. The two series match very well in the region $10<|z|<20$. Here $\Gamma(a)$ is the gamma function and $G(a,b,z)$ is given by the series

$$G(a,b,z)=1+\frac{ab}{1!z}+\frac{a(a+1)b(b+1)}{2!z^2}+\cdots\ . \quad (15)$$

The series expansions in the two regions have been verified by comparing with the Chebyshev expansion of $F(a,c,z)$,[17] with very good agreement. The Chebyshev expansion of $F(a,c,z)$ is valid for any value of z. However, it is not suitable for our purposes because of the difficulty of specifying beforehand the parameters of this representation that depend on the value of a, c, and z.

Numerical results obtained from Eq. (6) using Eqs. (10), (11), and (12) are given in Fig. 1. Atomic units are used in all of the figures. The real part of the self-energy for $r_s=2$, 4, and 6 is compared with the classical image potential. The same results are presented in Fig. 2 where the deviation of the quantum-mechanical results from the classical image potential is emphasized. At small distances quantum effects of electron recoil and surface-plasmon dispersion cause marked deviation of $\Sigma_0(z)$ from V_{cl}. It is interesting to show (Fig. 3) the contributions of the discrete and the continuum states to the image potential. The continuum states account for up to one-third of the total image potential and their contribution changes sign when z becomes large. However, this conclusion should not be taken too seriously here. A finite barrier surface model would be more reliable for handling the continuum.

The effect of dispersion of the surface-plasmon energy with the wave number is shown in Fig. 4. Dispersion is seen to weaken the image potential by almost 50% at $z=0$ for the electronic density $r_s=2$ compared with the result found neglecting dispersion. This is a considerably larger effect than reported by other researchers.[9] However, at large distances the two curves representing the results with and without dispersion approach one another because in such cases the electron couples effectively only to the long-wavelength surface modes.

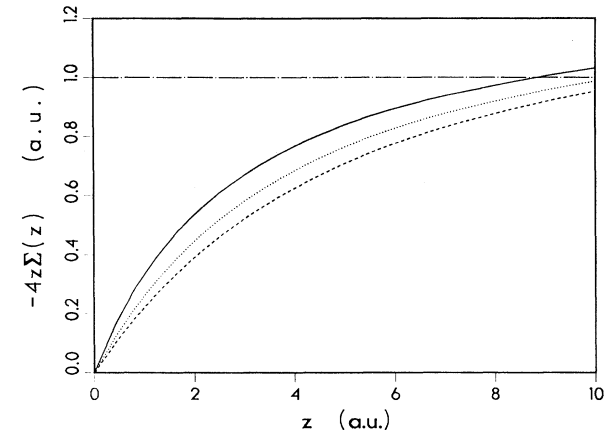

FIG. 2. The function $-4z\Sigma(z)$ is plotted here using the same results shown in Fig. 1. The deviation of the quantum-mechanical results from the classical image potential is emphasized here.

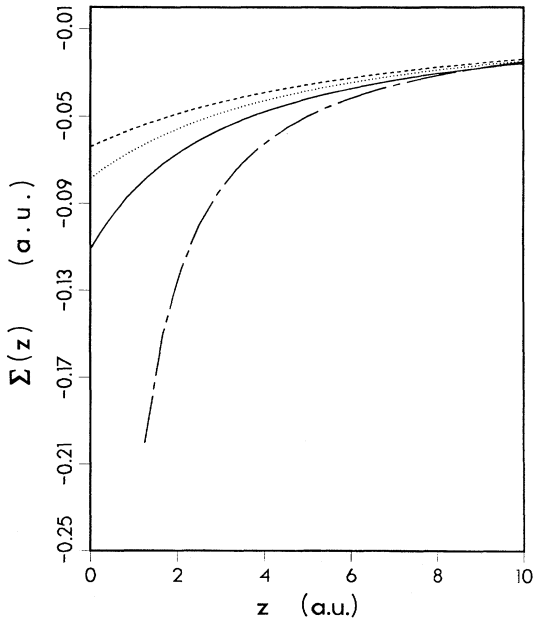

FIG. 1. Results of numerical evaluation of the self-energy for $r_s=2$, 4, and 6 compared with the classical image potential. The solid, dotted, and dashed lines corresponding to $r_s=2$, 4, and 6, respectively. The dot-dashed line represents the classical image potential.

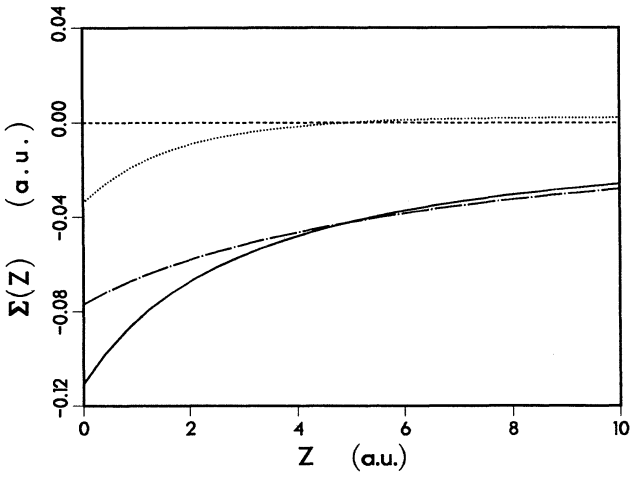

FIG. 3. Comparison of contributions to the total self-energy from the discrete and continuum states. The solid line stands for the total image potential. The dash-dotted line and the dotted line correspond to contributions from the discrete and continuum states, respectively. We take $r_s=2$ here.

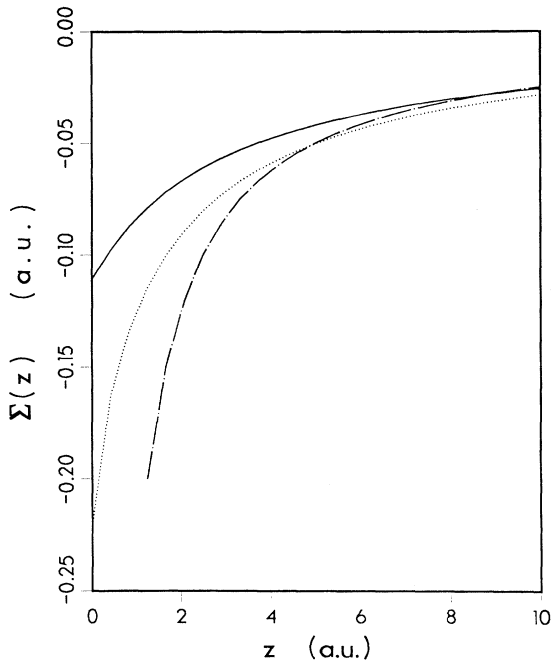

FIG. 4. Effects of surface-plasmon dispersion on the self-energy for $r_s=2$. The solid line shows the result with dispersion taken into account, the dotted line shows the results obtained neglecting dispersion, while the dot-dashed line shows $V_{\rm cl}$, the classical image potential.

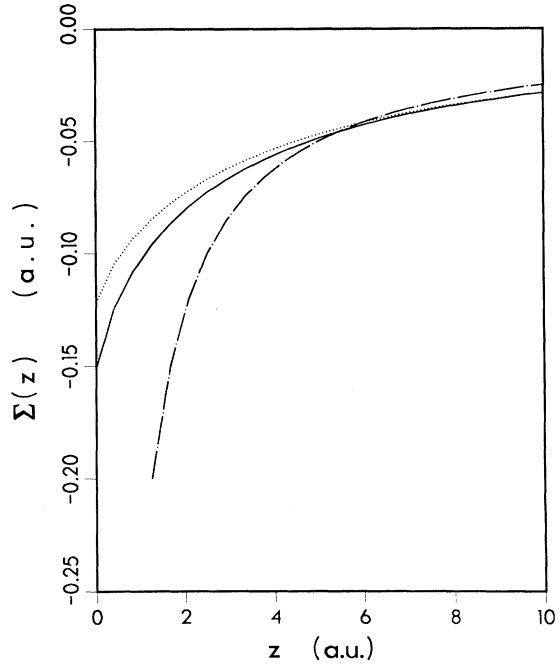

FIG. 6. The image potential obtained using dispersionless surface plasmons for $r_s=4$ (solid line), and $r_s=6$ (dotted line). The classical image potential is also shown as the dot-dashed line.

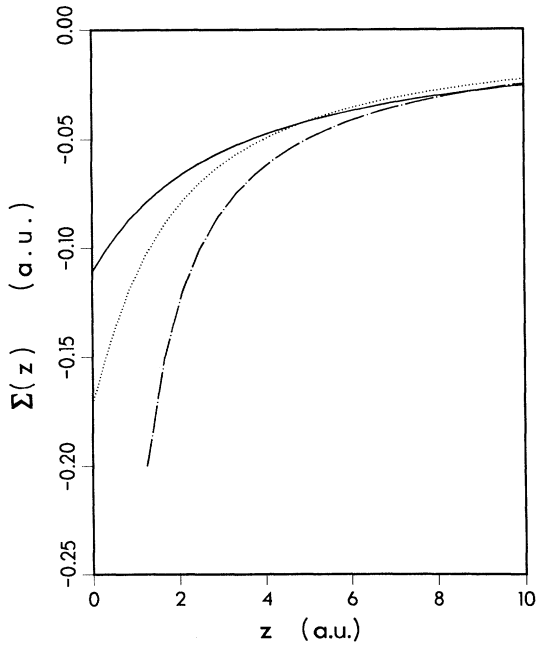

FIG. 5. Comparison of the self-energy obtained using a plane wave basis set (dotted line) and the Coulombic basis set (solid line) for $r_s=2$. The dot-dashed line shows the classical image potential. The surface-plasmon–pole dispersion relation was used in the evaluations.

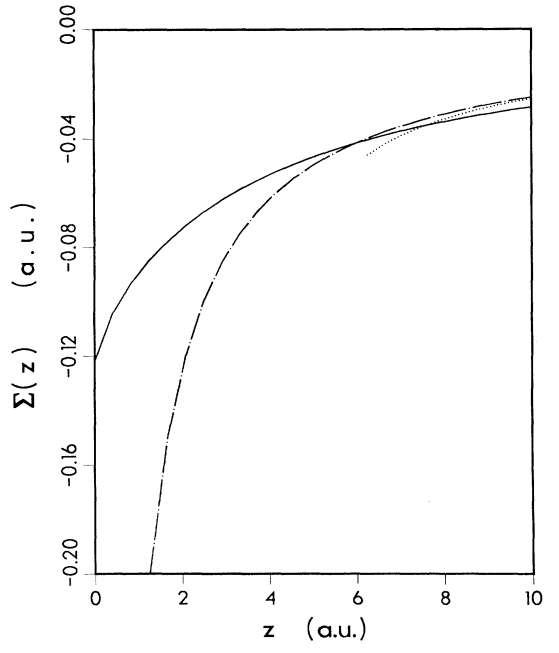

FIG. 7. Comparison of the second-order expression for the image potential using the Coulombic basis set, given by the solid line, with the higher-order image potential obtained using the plane wave basis set (Ref. 13) for $r_s=6$ (dotted line). The dot-dashed line stands for the classical image potential. Note that the results of Ref. 13 are valid only for $z \gg 1$.

It is interesting to see the dependence of the image potential on the particular basis set employed in the evaluation of Eq. (6). In Fig. 5 the image potential found using a plane-wave basis set is indicated by the dotted line. The result obtained using the Coulombic basis set, the solid line, shows that the image potential is weaker near the surface and stronger at large distances compared with the results found using plane waves. The surface-plasmon–pole dispersion relation, Eq. (12), was used in both calculations. The classical image potential is given by the dot-dashed line.

The dispersionless curve in Fig. 4 approaches the classical image potential from below. The same behavior is displayed for the electronic density parameter $r_s=4$ and 6 as shown in Fig. 6. This agrees generally with our previous analytical results found using high-order corrections to the image potential.[13] In Ref. 13 we employed a plane-wave basis set to evaluate the image potential up to the sixth order in perturbation theory. We showed there that at large distances the second-order result approaches the classical image potential and that the effects of high-order corrections are to strengthen the potential in this region. We believe that the second-order result found using the Coulombic basis set should be an improvement over results carried to the same order as given in Ref. 13. In Fig. 7 we give a comparison of the second-order result using the Coulombic basis set with results obtained using Eq. (11) of Ref. 13 in sixth-order perturbation theory. The latter are valid only for large z. Detailed comparisons are not appropriate here; the main point is that both basis sets predicts a strengthening of the image potential compared with $V_{\rm cl}$ when $z \gg 1$.

In summary, we have calculated the image potential experienced by an electron near a solid surface with an impenetrable wall using a self-energy formalism. Numerical results and discussions have been presented for an electron with zero initial momentum parallel to the surface. The dispersion of the surface plasmon is found to be responsible for the weakening of the image potential up to 50% at the surface compared with the result found including recoil but neglecting dispersion for conduction band densities corresponding to those in real metals.

The authors thank Professors P. M. Echenique, T. L. Ferrell, and J. R. Manson for helpful conversations. This research was sponsored by the Office of Health and Environmental Research, U.S. Department of Energy, under Contract No. DE-AC05-84OR21400 with Martin Marietta Energy Systems, Inc. and by the U.S.-Spain Joint Committee for Scientific and Technological Cooperation.

[1]E. Evans and L. D. Mills, Phys. Rev. B **8**, 4004 (1973).

[2]R. M. Nieminen and C. H. Hodges, Phys. Rev. B **18**, 2568 (1978); P. M. Echenique and J. B. Pendry, J. Phys. C **19**, 5437 (1986); A. Arnau and P. M. Echenique, Phys. Rev. B **35**, 7697 (1987); P. M. Echenique and J. B. Pendry, Prog. Surf. Sci. **32**, 111 (1989).

[3]X.-Y. Zheng, R. H. Ritchie, and J. R. Manson, Phys. Status Solidi B **157**, K-87 (1990).

[4]See, e.g., S. Anderson, Surf. Sci. **19**, 21 (1970); E. G. McRae and C. W. Caldwell, *ibid.* **57**, 63 (1976); **57**, 77 (1976); D. Straub and F. J. Himpsel, Phys. Rev. Lett. **52**, 1922 (1984); S. L. Hulbert, P. D. Johnson, and W. Weinert, Phys. Rev. B **34**, 3670 (1986). Reference 2 gives a more complete list of the references to experimental work.

[5]R. H. Ritchie, Phys. Lett. A **38**, 189 (1972); A. A. Lucas, Phys. Rev. B **4**, 2939 (1971); G. D. Mahan, *ibid.* **5**, 739 (1972); P. S. Feibelman, Surf. Sci. **27**, 438 (1981).

[6]P. M. Echenique, R. H. Ritchie, N. Barberan, and J. Inkson, Phys. Rev. B **23**, 6486 (1981).

[7]J. R. Manson and R. H. Ritchie, Phys. Rev. B **24**, 4867 (1981).

[8]A. G. Eguiluz and W. Hanke, Phys. Rev. B **39**, 10433 (1989).

[9]Also see, e.g., M. Sunjic, G. Toulouse, and A. A. Lucas, Solid State Commun. **11**, 1629 (1972); D. Chan and P. Richmond, Surf. Sci. **39**, 437 (1973); J. Harris and R. O. Jones, J. Phys. C **6**, 3585 (1973); J. Heinrichs, Phys. Rev. B **8**, 1346 (1973); M. Jonson, Solid State Commun. **33**, 743 (1980).

[10]Z. Penzar and M. Sunjic, Phys. Scr. **30**, 431 (1984).

[11]J. R. Manson and R. H. Ritchie, Phys. Rev. Lett. **54**, 785 (1985).

[12]J. R. Manson, R. H. Ritchie, and T. L. Ferrell, Phys. Rev. B **29**, 1080 (1984).

[13]X.-Y. Zheng, R. H. Ritchie, and J. R. Manson, Phys. Rev. B **39**, 13510 (1989).

[14]X.-Y. Zheng and R. H. Ritchie (unpublished).

[15]R. Shakeshaft and L. Spruch, Phys. Rev. A **31**, 1535 (1985).

[16]L. D. Landau and E. M. Lifshitz, *Quantum Mechanics, Non-Relativistic Theory,* 3rd ed. (Pergamon, Oxford, 1977).

[17]Y. L. Luke, *Algorithms for the Computation of Mathematical Functions* (Academic, New York, 1977).